

Radiative decay of vacuum-ultraviolet excitation of silica synthesized by molecular precursors of Si-Si sites: An indicator of intracenter relaxation of neutral oxygen vacancies

A. Paleari,* N. Chiodini, D. Di Martino, and F. Meinardi

Istituto Nazionale Fisica della Materia, Dipartimento di Scienza dei Materiali, Università di Milano-Bicocca, via Cozzi 53, I-20125 Milano, Italy

(Received 21 May 2004; revised manuscript received 27 September 2004; published 1 February 2005)

A well defined type of oxygen deficiency has been induced in the silica network by introducing Si-Si groups through a molecular doping based on the sol-gel synthesis. In this material, we have investigated the visible and UV photoluminescence (PL), up to 7 eV, arising from localized states excited in the energy range 3–12 eV by synchrotron radiation. The PL excitation spectrum is dominated by one main sub-band-gap excitation band, peaked at 7.1 with a full width of half-maximum of 0.8 eV. No PL arises exciting at 5 eV, specifically no PL band at 4.4 and 2.7 eV are observed, ruling out the formation of twofold coordinated -Si-sites. These data confirm all previous theoretical and experimental assignments of transitions at about 7–8 eV to localized excitations of neutral-oxygen-vacancy (NOV) sites. Exciting in the vacuum-UV (VUV) above 7 eV, the investigated material does not show the typical 4.4 and 2.7 eV PL observed in fused silica. The peculiar NOV configuration appears to inhibit the photoconversion process responsible in fused silica for the VUV excitation of the twofold coordinated silicon emission. The main emission is peaked at about 3.7 eV, with a PL lifetime of about 1 μ s. A minor component with a much slower lifetime (800 μ s) has been detected at 2.9 eV, with a further minor excitation channel at about 6 eV. All emissions excited at 7.1 eV show an intensity decrease with the temperature, but a negligible thermal change of the lifetime. The results give an indication of the possible energy level structure of NOV and evidence an efficient nonradiative decay mechanism of the excited state, caused by a strong electron-phonon interaction during the VUV excitation of the defect. The analysis of the data suggests a large Si-Si bond relaxation of about 0.1 nm, giving definite experimental confirmation of previous theoretical calculations.

DOI: 10.1103/PhysRevB.71.075101

PACS number(s): 78.55.Qr, 81.20.Fw

I. INTRODUCTION

Silicon-silicon covalent bonds in the 4:2 coordination structure of silicon dioxide are among the key defect configurations responsible for defect-related processes in SiO₂, many of them with a demonstrated technological relevance. Point defects play an important role in several optical applications of silica, such as in photorefractive writing of optical waveguides and in vacuum-ultraviolet (VUV) photolithography.^{1–3} Nevertheless, the attribution of the optical features arising from point defects are still debated.^{4,5} Quite surprisingly, a major uncertainty concerns the identification of transitions pertaining to the neutral oxygen vacancy (NOV) in the form of $\equiv\text{Si}-\text{Si}\equiv$ sites, which is expected to be the basic and more abundant intrinsic defect in the silica network. Optical absorption at 7.6 eV in oxygen deficient or neutron irradiated silica is almost consensually⁵ attributed to excitation of this site from its ground-state S_0 singlet to an excited S_1 state. This attribution is based on experimental and theoretical evidence.⁴ Alternative assignments were proposed earlier⁵ and more recently.^{6,7} Further complications come from controversial assignments of the emission bands observed by excitation at 7.6 eV: a fast 4.4 eV (few ns decay time) and a slow (about 10 ms of decay time) 2.7 eV photoluminescence (PL) bands. These emissions are excited within PL excitation (PLE) bands at 5 and 6.9 eV, and also in agreement with a four-level intracenter scheme comprising three singlet states S_0 , S_1 , and S_2 , and a triplet T_1 level. The $S_0 \rightarrow S_1$ and $S_0 \rightarrow S_2$ transitions are responsible for excitation

bands at 5 and 6.9 eV PL, respectively, while PL at 4.4 and 2.7 eV are assigned to $S_1 \rightarrow S_0$ and $T_1 \rightarrow S_0$ transitions, respectively. In this scheme, the 7.6 eV band was initially interpreted as caused by transitions to a further excited state of the same defect, with a $\equiv\text{Si}-\text{Si}\equiv$ configuration.⁸ However, successive studies, with detailed consideration of the kinetics of the PL decay processes excited at 5, 6.9, and 7.6 eV, resulted in a new scenario with two kinds of oxygen-deficient centers (ODCs), named ODC(I) and ODC(II), absorbing at 7.6 and 5 eV, respectively.⁹ A few studies investigated the possible attribution of ODC(I) and ODC(II) to relaxed $\equiv\text{Si}-\text{Si}\equiv$ and unrelaxed $\equiv\text{Si}\cdots\text{Si}\equiv$ sites, respectively,¹⁰ also by means of theoretical calculations.^{11–14} More recently, during the last decade, Skuja¹⁵ proposed a completely different ODC(II) model, now widely accepted, where the phenomenological scheme of the 5 and 6.9 eV excited PL, with all implications on lifetimes, temperature dependence of relative intensities, and cation-substitution effects on transition rates, is well accounted for by a twofold-coordinated -Si- configuration,^{4,16} whose C_{2v} local symmetry is also consistent with polarization-sensitive PL measurements.¹⁷ *Ab initio* calculations have recently confirmed this proposal.^{18,19} However, the upgraded interpretation of ODC(II) further complicated the assignment of the ODC(I) optical activity. In fact the problem arose of explaining the coincident PL features excited at 7.6 and 5 eV. A model of defect conversion upon 7.6 eV excitation from $\equiv\text{Si}-\text{Si}\equiv$ sites to -Si- configuration, with a possible nonradiative decay towards two E' centers (i.e., unpaired sp^3 elec-

trons in threefold coordinated $\equiv\text{Si}\cdot$ sites) was proposed by Skuja¹⁵ and then theoretically demonstrated by molecular dynamic (MD) simulations.²⁰ From an experimental point of view, detailed measurements²¹ have recently confirmed that an intersystem process is involved in the 7.6 eV excited 4.4 eV PL. On the other hand, recent numerical calculations by embedded density-functional theory of configuration energy suggest possible intracenter PL from T_1 and S_1 states of $\equiv\text{Si}-\text{Si}\equiv$ sites in the same energy range of emissions from $-\text{Si}-$ sites, although with a large energy uncertainty.^{12–14} In addition, the previously quoted MD study²⁰ gives a non-null activation energy for the defect conversion from $\equiv\text{Si}-\text{Si}\equiv$ to $-\text{Si}-$ sites. Even if its value (0.72 eV) is probably overestimated, this suggests a possible intracenter decay, and it is not clear whether it is superimposed on the $-\text{Si}-$ emissions or strongly inhibited by the occurrence of a largely more favored photoconversion of the $\equiv\text{Si}-\text{Si}\equiv$ site. In fact, no intracenter radiative decay from ODC(I) has yet been identified as free from interference with optical activity ascribable to stable or transient ODC(II). As a consequence, the energy structure and the occurrence itself of NOV centers have remained elusive.

In this work, we have found a way to force $\equiv\text{Si}-\text{Si}\equiv$ sites into a configuration that prevents the occurrence of ODC(II), either as native or transient defects from NOV photoconversion. This result gives evidence for the sensitivity of the photoconversion process to the defect environment, and gives also an insight into the possible NOV transitions and energy structure of this basic defect in silica.

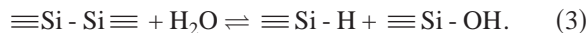
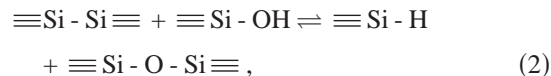
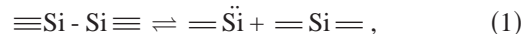
II. EXPERIMENT

A. Material synthesis and treatments

The choice of the kind of material synthesis was crucial in this work to obtain a system enabling the investigation of a particular kind of oxygen deficiency. To ensure the introduction of the specific NOV configuration, synthesis of silica by the sol-gel method was used. This method starts from room temperature hydrolysis of molecular precursors of the silica SiO_4 tetrahedral units, specifically $\text{Si}(\text{OCH}_2\text{CH}_3)_4$ (TEOS), forming a low-density skeleton that is successively purified from solvents and organic radicals, as well as dried and densified, through a slow thermal treatment in controlled atmosphere (usually in a flux of oxygen) up to about 1000 °C.²² In this way, ethyl and methyl groups are removed (even below 500 °C), as well as possible carbonyl residuals. Pure silica with the typical density of vitreous silica is finally obtained, with a content of OH groups of the order of 0.1 at. %.

In the first step of the synthesis, other molecular reagents may be introduced together with TEOS to achieve complex compositions or doping of the silica matrix. The hexamethoxydisilane (EMODS) $\text{Si}_2(\text{OCH}_3)_6$ molecule, containing the $\equiv\text{Si}-\text{Si}\equiv$ group, can be used to introduce NOV sites in the silica network, provided that a suitable inert atmosphere prevents complete oxidation of the material, comprising all Si-Si bonds, during the thermal treatment. However, even in an inert atmosphere, $\equiv\text{Si}-\text{Si}\equiv$ sites may react and convert into other coordination structures during the thermal treat-

ment, especially within a highly hydrated low-density matrix. Specifically, care should be taken to account of the possible occurrence of reactions, in principle chemically feasible, such as



Reaction (1) expresses the possibility of the thermally activated reaction of defect conversion between ODC(I) and ODC(II), analogous to the VUV excited defect conversion of ODC(I) decaying in ODC(II) proposed to explain the excitation of ODC(II) PL within the ODC(I) absorption band.^{15,20} Occurrence of this reaction would compromise the selectivity of the synthesis method in doping with ODC(I) only. Checking the absence of PL from ODC(II), we verified that the equilibrium of reaction (1) is largely unbalanced towards ODC(I) throughout the synthesis route, confirming that $\equiv\text{Si}-\text{Si}\equiv$ sites from EMODS are stable as regards reaction (1). Reactions (2) and (3) may instead be really efficient during the thermal treatment in removing a major fraction of the $\equiv\text{Si}-\text{Si}\equiv$ sites introduced by the synthesis, because of the great amount of OH groups and adsorbed water in the first steps of the sol-gel preparation method. In fact, hydroxyl groups and water molecules are highly reactive in silicon dioxide, as experimentally and theoretically proved.^{23–25} Reaction (3) has been recently studied by first-principles calculations.²⁵ To verify that the equilibrium of reactions (2) and (3) is not completely unbalanced towards the formation of $\equiv\text{Si}-\text{H}$ sites, a parallel synthesis of samples from TEOS with addition of triethoxysilane (TREOS) $\text{Si}(\text{OCH}_2\text{CH}_3)_3\text{H}$, containing $\equiv\text{Si}-\text{H}$ groups, was carried out. In fact, if a fraction of $\equiv\text{Si}-\text{Si}\equiv$ sites is stable as regards reaction (2) throughout the synthesis route, the material resulting from addition of TREOS should contain $\equiv\text{Si}-\text{Si}\equiv$ sites as well. Anyway, amounts of EMODS or TREOS of few mol % were used to assure a less than complete reaction with hydroxyl groups in the final high-temperature steps of the treatment, when OH content drops at smaller values. Therefore, oxygen deficient silica samples were prepared by co-gelling TEOS and 1 or 5 mol % of EMODS or TREOS in ethanol, as a solvent, by adding H_2O (TEOS/ H_2O 1:8 molar ratio, TEOS/ethanol 1:3 volume ratio). Gelation occurred in a few days at 40 °C. Xerogel was then obtained by slowly evaporating the solvent. The final transparent glass has been produced by heating in inert atmosphere N_2 or Ar (4 °C/h) up to complete densification at 1050 °C. Reference samples from TEOS were also synthesized for comparison.

B. Optical measurements

PL measurements were carried out using synchrotron radiation at the SUPERLUMI experimental station of HASYLAB at DESY (Hamburg, Germany), in the temperature range between 9 and 300 K. The excitation spectral band-

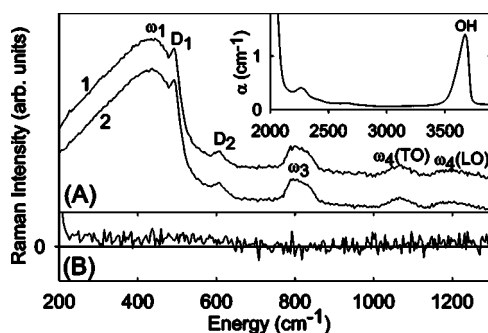


FIG. 1. (a) Raman spectra at 300 K of silica produced by the sol-gel method with addition of EMODS (curve 1) and commercial synthetic pure silica (Tetrasil B, Haereus) (curve 2). Spectra are shifted for clarity. (b) Difference spectrum (curve 2–curve 1). Inset: infrared spectrum of silica produced by the sol-gel method with addition of EMODS.

width was 0.3 nm with photon energy ranging between 5 and 12 eV. PL signals were detected by a photomultiplier coupled with monochromators with 3 nm of emission bandwidth up to 5 eV, and 0.5 nm up to 7.5 eV in a vacuum chamber. Data were corrected for the spectral dependence of the excitation intensity. Time resolved measurements in the nanosecond domain were carried out with a time window of 200 ns and 0.8 ns overall time response. Slow PL decays were measured by chopping the excitation with a time window of 20 or 500 μ s and 1 or 25 μ s of pulse rise time, respectively. Lifetime values were calculated by fitting decay curves as a convolution of contributions from exciting pulse and emission decay.

III. RESULTS

A. Material characterization

Analysis of the main physical and structural features of the final material was carried out through measurements of refractive index (using the prism-coupler technique), porosity (with the Bnanauer-Emmett-Taylor method), Raman analysis, visible and IR absorption, and electron paramagnetic resonance (EPR) measurements. We found a refractive index value $1.45705 \pm 8 \times 10^{-5}$ at 633 nm, to be compared with $1.45702 \pm 3 \times 10^{-5}$ of commercial pure silica.²⁶ This value is consistent with the transformation of the xerogels into glass after the thermal treatment at 1050 °C, as expected from this kind of route.²² Measurements of surface area after the thermal treatment did not give values above the sensitivity limit (1 m²/g). The Raman spectrum in the phonon energy range 200–1300 cm^{−1} [curve 1 in Fig. 1(a)], with broad structures centered at 440, 800, and 1050–1200 cm^{−1} (ω_1 , ω_3 , and ω_4 modes, respectively) and peaks at 495 and 606 cm^{−1} (D_1 and D_2 peaks, respectively), reproduces the typical features of pure silica.²⁷ These data reflect the formation of a glassy network without crystallization or spurious phases.^{28,29} The comparison with the spectrum of a commercial pure silica [curve 2 in Fig. 1(a)] does not show significant deviations [difference spectrum in Fig. 1(b)]. The IR spectrum [inset of Fig. 1(a)] rules out the presence of organic

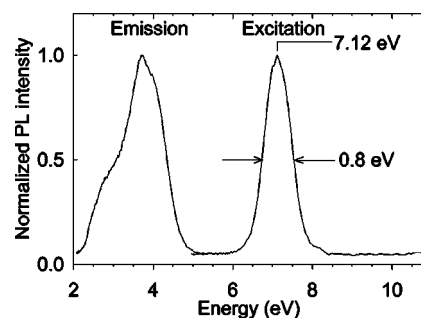


FIG. 2. 10 K PL spectrum excited at 7.1 eV in NOV-doped silica produced by the sol-gel method, and PL excitation spectrum of PL at 3.7 eV.

residuals of the solgel synthesis in form of ethylic or methylic groups, whose vibrational modes should give narrow peaks in the range 2800–3000 cm, but only a relevant concentration of Si-OH sites. Visible and near-UV absorption spectra from 800 to 200 nm and EPR measurements of samples of the final material did not evidence any detectable optical or paramagnetic activity from metallic or other impurities or intrinsic color centers, showing completely flat spectra.

B. Photoluminescence

Analysis of PL activity was carried out collecting PL spectra at several excitation energy values in the range 5–8 eV to identify the defect-related sub-band-gap excited emissions of the silica glass investigated. Excitation at energy higher than the gap of silica was also carried out at 11 eV. This analysis, throughout a set of different samples synthesized from TEOS, TEOS and EMODS, and TEOS and TREOS, evidenced one kind of PL activity, efficiently excited at around 7 eV. This activity is completely absent in undoped silica samples produced via the same route from TEOS only. No sample exhibits PL excited at around 5 eV, ruling out the formation of ODC(II).

The observed emission is peaked at 3.7 eV, with a shoulder at about 2.9 eV, and an excitation band peaked at 7.12 eV with a bandwidth of about 0.8 eV [full width at half-maximum (FWHM)] (Fig. 2). Possible PL components in the VUV up to 7 eV were also looked for, using a different detection line, but no other emission was found.

Significant intensity changes were observed changing the temperature, as shown in Fig. 3(a). Specifically, the PL intensity, irrespective of the emission energy, grows following the temperature dependence shown in Fig. 3(b). By contrast, distinct PL lifetime τ values pertain to the PL components. A longer PL decay ($\tau \approx 800 \mu$ s) is observed for the minor component at 2.9 eV, whereas a lifetime of about 1 μ s has been estimated for the emission at 3.7 eV. No relevant change of lifetime was observed increasing the temperature.

The bandwidth of the excitation spectrum (0.78 eV at 8 K) shows a small thermal broadening of 0.07 eV when heating the sample to 300 K [Fig. 4(a)]. Such a large temperature-independent bandwidth indicates either a strong electron-phonon interaction or a large inhomogeneous con-

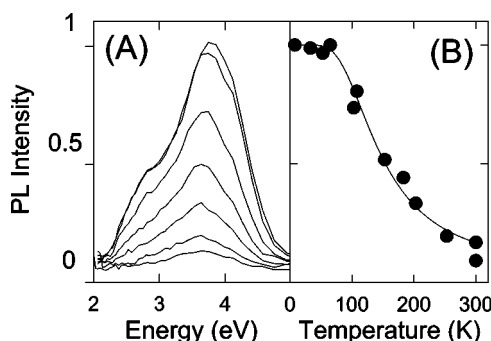


FIG. 3. (a) PL spectra excited at 7.1 eV in NOV-doped silica produced by the sol-gel method and densified up to 1050 °C at different temperatures from 8 K to 300 K (with intensity decreasing by increasing the temperature) in steps of about 50 K. (b) Temperature dependence of the PL intensity. The curve is the best fit from Eq. (7).

tribution. To investigate this aspect, we have collected excitation spectra at different emission energies [Fig. 4(b)], showing no significant modification of the spectral shape as instead expected from an inhomogeneously broadened band. Figure 4(b) also shows a much less efficient excitation channel at about 6 eV, with a relatively larger yield for the 2.9 eV PL component. No relevant change of intensity appears by changing the temperature at this excitation energy.

IV. DISCUSSION

A. Origin of the PL activity

Our data show that a VUV PLE activity at 7.1 eV is induced in silica as a result of the molecular doping with precursors of $\equiv\text{Si}-\text{Si}\equiv$ groups. The careful consideration of the possible reactions involving $\equiv\text{Si}-\text{Si}\equiv$ precursors during the networking and densification of the silica matrix (Sec. II A) suggests to ascribe the PL activity to $\equiv\text{Si}-\text{Si}\equiv$ sites in form of intrinsic defects. This is supported by the comparison between doped and undoped samples, and by the physical and structural analysis of the final material. In fact, the 7.1 eV PLE is absent in undoped (from TEOS only) silica

produced by analogous sol-gel preparation method, with comparable probability of contamination from impurities due to either the reagents or the process. Therefore, the 7.1 eV PLE cannot be ascribed to impurities or extrinsic residuals of the synthesis process. The analysis of the physical and structural properties (Sec. III A), in agreement with other studies on sol-gel silica,²² confirms that the sol-gel route, after a thermal treatment at temperature higher than 1000 °C, gives rise to the formation of a fully inorganic matrix of amorphous SiO_2 with a purity level comparable with commercial synthetic pure silica. Raman data, together with refractive index and surface area measurements, show typical bulk features without detectable evidence of a porous matrix.^{28,29} Therefore, surface defects are unlikely to be responsible for the observed PL activity. As a matter of fact, PL emissions of porous silica or silica xerogels^{30–33} show PL bands in the spectral region 2–4 eV, but with small Stokes shift (0.5–2 eV) from the excitation and fast PL decay time in the nanosecond domain, in contrast with the excitation and lifetime features of our data. Anyway, the optical activity of porous silica-based materials typically vanishes after thermal treatment at about 1000 °C.³³

In summary, the strategy of synthesis, the material characterization, the measurements of reference samples, and the consideration of previous works on sol-gel silica, point to the assignment of the 7.1 eV optical transition to the excitation of intrinsic defects, specifically to $\equiv\text{Si}-\text{Si}\equiv$ sites introduced by molecular doping in an otherwise pure silica network.

This result is in agreement with all previous theoretical and experimental attributions of VUV excitation transitions above 7 eV to NOV's. Nevertheless, the approach we have followed to induce NOV sites gives rise to a PL phenomenology with three main peculiarities: (i) no optical activity is observed from ODC(II) decay, neither native nor generated from photoactivated conversion of VUV excited ODC(I); (ii) VUV excitation gives rise to previously unobserved radiative decay channels; and (iii) the VUV PLE band related to NOV is slightly different in energy with respect to the band usually attributed to ODC(I) and found in the range 7.4–7.6 eV.

The observed peculiarities are evidence of the possibility of obtaining a NOV environment significantly different from that arising in silica produced at high temperature. As regards the lowering of the excitation energy, the shift is comparable with that encountered in other silica defects occurring in different variants as a result of environment modifications, such as bulk and surface E' centers (from 5.8 to 5.4 eV) and native/extrinsic and radiation-induced ODC(II) (from 5.2 to 4.9 eV).^{4,34} Indeed, theoretical cluster calculations³⁵ of the NOV energy structure showed that a slight modification of configuration constraints in the shell of the six coordinating oxygen atoms, with a resulting change of the Si—Si distance of only 5×10^{-3} nm, is sufficient to decrease the $S_0 \rightarrow S_1$ transition energy of 0.4 eV. Therefore, particular structural constraints, deriving from the molecular introduction of Si-Si sites via the sol-gel method, can really justify a significant shift of the NOV excitation.

The lowering of transition energy from 7.6 down to 7.1 eV is consistent with an excited NOV level deeper in the gap and a more localized charge density of the excited configuration. Therefore, the strong Rydberg feature of the VUV

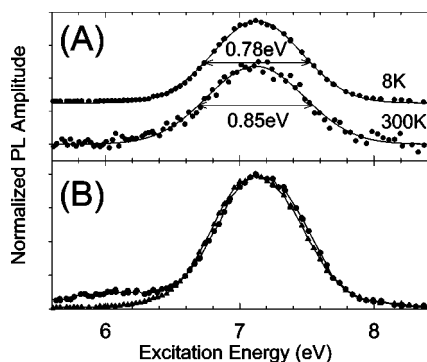


FIG. 4. (a) Excitation spectra of the 3.7 eV emission in NOV-doped silica at 8 and 300 K. Solid curves are Gaussian fit of the data giving the indicated FWHM values. (b) 8 K excitation spectra of PL at 2.7 (circles) and 3.7 eV (triangles).

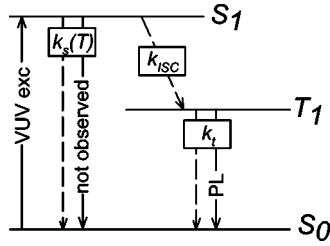


FIG. 5. Schematic of transitions induced by VUV excitation involving singlet (S) and triplet (T) states of NOV sites. Radiative (nonradiative) transitions are indicated by solid (dashed) arrows with the respective rate constants [Eqs. (4)–(6)].

$S_0 \rightarrow S_1$ transition, evidenced by different theoretical studies,^{11,12,20} should be reduced in molecularly induced NOV. A significantly higher potential barrier is thus expected for configuration changes, in agreement with the lack of NOV-to-ODC(II) photoconversion in our samples. Preliminary MD calculations³⁶ confirm the possibility of NOV configurations with a barrier higher than 2 eV.

B. Scheme of radiative transitions

The results in Figs. 2 and 3, together with lifetime τ values, give an indication of the decay paths of this NOV variety. The lifetime values indicate a small transition probability from the emitting levels (T_1 states) towards the ground state, consistent with partially forbidden triplet-to-singlet $T_1 \rightarrow S_0$ transitions. In contrast, no fast $S_1 \rightarrow S_0$ radiative decay, expected in the nanosecond domain, is observed, indicating that strongly competitive decay channels are active from the 7.1 eV excited S_1 level. One of these is directed towards the T_1 levels responsible for the 2.9, 3.7 eV PL emissions (Fig. 5). However, another competitive process is active, consisting of an efficient nonradiative decay to the ground state, favored by the temperature, and competitive with the intersystem crossing (ISC) process $S_1 \rightarrow T_1$ as well. In fact, the PL intensity from $T_1 \rightarrow S_0$ turns out to be strongly dependent on the temperature without a comparable effect on the PL lifetime. The PL intensity decreases by more than a factor of 10 heating from 10 to 300 K, but no detectable change of τ is observed, ruling out that nonradiative decays of T_1 states could have a relevant role in the change of emission intensity. In addition, the ISC $S_1 \rightarrow T_1$ process does not appear significantly phonon assisted, unlike the ODC(II) defect configuration, since no evidence is observed for a positive contribution to the PL intensity by increasing the temperature. Emission from T_1 levels by exciting at 6 eV might reflect the radiative decay of the forbidden $S_0 \rightarrow T_1$ excitation. The very low intensity did not allow us a detailed spectral analysis and no reliable value of PL lifetime could be estimated by exciting at 6 eV. In any case the attribution to PL excited by the $S_0 \rightarrow T_1$ transition is supported by the thermal behavior of the PL intensity, which does not show relevant changes in the investigated temperature range, as expected on the basis of the lack of temperature dependence of τ by exciting at 7.1 eV.

In this scheme, the PL emissions around 2.5–4 eV give an indication of the energy position of the triplet state with

respect to the ground level of the site. Indeed, previous theoretical studies on the NOV configuration in silica suggested a triplet state of the site with excitation energy of about 4–6 eV and relaxation energy of the excited state of about 2 eV, resulting in a triplet-to-singlet transition energy ranging from 1 to 4 eV. This was found by MD, Hartree-Fock, or configuration interaction calculations.^{11,12,14,20} Our data indeed confirm the possibility of intracenter radiative decays of NOV sites and give an experimental basis for a quantitative refinement of further calculations.

C. Effects of the temperature

As discussed in the previous section, the thermal behavior of I_{PL} reflects the temperature dependence of the competitive nonradiative decay of S_1 to the ground state, which in turn is related to the vibrational properties of the excited state. To investigate this aspect, the thermal behavior of the PL intensity (inset of Fig. 3) may be analyzed starting from the kinetics of excitation and decay of the NOV site:

$$\frac{d}{dt}n_s = k_0n_0 - (k_s + k_{ISC})n_s, \quad (4)$$

$$\frac{d}{dt}n_t = k_{ISC}n_s - k_t n_t, \quad (5)$$

where n_0 , n_s , and n_t are the populations of NOV in the S_0 , S_1 , and T_1 states, respectively, while k_s , k_t , and k_{ISC} are the total rate constants (accounting for both radiative and nonradiative transitions) of S_1 and T_1 decays towards the ground state and of the IST transition from S_1 to T_1 levels, respectively, as indicated in Fig. 5. In this scheme, in the stationary state, the intensity of PL emission is proportional to the population n_t of the radiative T_1 levels, and dependence of n_t upon the rate constants can be obtained:

$$n_t \propto \frac{k_{ISC}}{k_s + k_{ISC}} \frac{k_0}{k_t} n_0. \quad (6)$$

As discussed in the previous section, the lifetime measurements and the decrease of PL at high temperature suggest that the thermal dependence of k_t and k_{ISC} is negligible. Therefore, in Eq. (6), the temperature dependence of n_t , determining the thermal behavior of PL intensity, arises from k_s . The explicit dependence on the temperature can be evidenced through the expression of the temperature dependence of the rate constant k_s dominated by the nonradiative decay of the S_1 level to the ground state. The temperature dependence of the rate constant k_s may be approximately described by an expression derived by Mott's activation-energy law³⁷ $k_s \propto \exp(-E_a/kT)$ with a temperature dependent activation energy $E_a = B - \langle n \rangle_T$ where B is the potential barrier for the nonradiative process from the minimum energy of the excited state and $\langle n \rangle_T$ is Planck's thermal average phonon number $[\exp(h\nu/kT) - 1]^{-1}$ to take into account the thermal dependence of the phonon contribution to the excited state energy (with effective phonon energy $h\nu$) in a configurational-coordinate approach.³⁸ As a consequence, the temperature dependence of PL intensity I_{PL} , proportional to n_t given by Eq. (6), takes the form

$$I_{PL} \propto \frac{1}{1 + A \exp[-(B - \langle n \rangle_T)/kT]}. \quad (7)$$

The fit of data in Fig. 3(b) using Eq. (7) gives an energy barrier B for the nonradiative process of 0.04 eV and an effective energy $h\nu$ of the phonon modes of about 410 cm^{-1} . This value matches well the energy of about 430 cm^{-1} of the stretching mode of the Si-Si bond.³⁹

D. Electron-phonon interactions

The values of phonon energy and activation barrier obtained from the kinetic model of $I_{PL}(T)$ can furnish an approximate evaluation of the electron-phonon interactions responsible for the peculiar nonradiative processes at NOV defects. The lack of data on the energy of the radiative decay prevents a quantitative analysis in terms of a detailed configurational-coordinate model. In any case, the B value of the barrier for nonradiative decays may be viewed as the energy from the minimum of the excited level to the crossover of the potential curves of the two states.³⁸ Taking the phonon energy $h\nu$ in the range $410\text{--}430 \text{ cm}^{-1}$ and the excitation energy E_{exc} at 7.1 eV, the energy B for the crossover between the levels may be related to an effective Huang-Rhys factor λ^2 that gives a measure of the relaxation energy of the excited site in phonon energy units $h\nu$:

$$E_{exc} - \lambda^2 h\nu + B = \lambda^2 h\nu [1 + (B/\lambda^2 h\nu)^{1/2}]^2, \quad (8)$$

where the left side describes the excited state potential at the crossover, while the right side is the crossover energy along the ground-state potential curve. Equation (8) gives $\lambda^2 \approx 60$, reflecting a large electron-phonon interaction. In this case, broad bands are expected from a large site relaxation upon excitation. The bandwidth (FWHM) is given by $\Delta E = 2.35h\nu\lambda(1+\beta)/(1-\beta)$, where $\beta = \exp(-h\nu/kT)$ is the Boltzmann factor. From the estimated values λ^2 and $h\nu$, we obtain $\Delta E \approx 0.9 \text{ eV}$ in the low-temperature limit ($\beta=0$), with an expected thermal broadening of about 0.1 eV at 300 K. This is close to the experimental bandwidth of 0.8 eV and the small thermal broadening of 0.07 eV barely observed just above the experimental uncertainty (Fig. 4). The agreement, even though within the crude approximation of the model, suggests a relevant relaxation of the excited configuration. If the nonradiative decay were not so efficient as the small B value shows, a PL emission with a relevant Stokes shift $2\lambda^2 h\nu \approx 6 \text{ eV}$ would be expected. Experiments to detect possible infrared emissions at lower temperature by exciting at 7.1 eV might clarify this aspect, but the competitive decay of the S_1 state through T_1 levels is expected to prevent observation of the $S_1 \rightarrow S_0$ radiative decay. In any case, another important parameter can be obtained from the semiquantitative evaluation of the electron-phonon interaction of NOV

sites, specifically the Franck-Condon offset Δd between the configurational coordinates of the two states in their relaxed configurations. In fact $a=2\lambda$ (with a value of about 16) is the dimensionless measure of the offset between the minima of S_1 and S_0 in units of zero-point-vibration amplitude x_v . Since the relevant phonon energy resulting from our analysis matches the energy of the stretching mode of the Si-Si bond, we may suppose that the relevant configurational-coordinate is approximately related to the stretching of the Si-Si bond, while the vibrational amplitude x_v depends on the reduced mass μ of the Si-Si group through the expression $x_v^2 = \hbar^2/h\nu\mu$. From x_v and a , the excitation-related relaxation of NOV site results in an offset Δd_{Si-Si} of about 0.12 nm, which is a large distortion compared with the equilibrium Si-Si bond length of 0.24–0.26 nm.³⁹ Our approximate evaluation of Δd_{Si-Si} is indeed consistent with theoretical calculations: MD calculations²⁰ found a relaxation of 0.07 nm consequent to excitation to the triplet NOV state, suggesting even larger relaxation of the excited S_1 state. In fact, cluster calculations¹¹ of the excited S_1 state found that Si atoms move 0.36 nm apart after NOV excitation, resulting in $\Delta d_{Si-Si} \approx 0.11 \text{ nm}$, in good agreement with our analysis.

V. CONCLUSIONS

The controversial question of the energy structure and intracenter transition scheme of NOV in silica, complicated until now by the proven occurrence of concomitant photoactivated intercenter processes, has been experimentally disentangled by forcing molecular Si-Si precursors in a network, preventing the ODC(I)→ODC(II) photoconversion. Evidence for the intracenter energy structure of the NOV configuration has been obtained, giving an experimental basis for all previous calculations of the $S_0 \rightarrow S_1$ and $T_1 \rightarrow S_0$ NOV transitions, as well as of the environment sensitivity of the ODC(I)-to-ODC(II) interconversion mechanism. A prominent role of the site relaxation upon excitation to the S_1 state is strongly supported by the analysis of our data. The huge excitation-induced relaxation represents the main peculiarity of NOV sites, probably the crucial feature for several aspects involving defect photoactivated processes in silicon dioxide.

ACKNOWLEDGMENTS

The authors thank Simone Agnello for fruitful comments and discussion. They also thank Marco Bernasconi and Marco Cannas for making available theoretical and experimental unpublished results, respectively. This work is part of a National Project partially supported by the Italian Government. Experiment at HASYLAB was supported by the IHP Contract No. HPRI-CT-1999-00040/2001-00140 of the European Commission.

*Electronic address: alberto.paleari@mater.unimib.it

- ¹J. Albert, MRS Bull. **23**, 36 (1998).
- ²M. J. Dejneka, MRS Bull. **23**, 57 (1998).
- ³W. Margulis, F. C. Garcia, E. N. Hering, L. C. Guedes Valente, B. Lesche, F. Laurell, and I. C. S. Carvalho, MRS Bull. **23**, 31 (1998).
- ⁴L. Skuja, in *Defects in SiO₂ and Related Dielectrics: Science and Technology*, edited by G. Pacchioni, L. Skuja, and D. L. Griscom (Kluwer Academic, Dordrecht, 2000), p. 73.
- ⁵D. L. Griscom, J. Ceram. Soc. Jpn. **99**, 899 (1991).
- ⁶A. N. Trukhin, in *Defects in SiO₂ and Related Dielectrics: Science and Technology*, edited by G. Pacchioni, L. Skuja, and D. L. Griscom (Kluwer Academic, Dordrecht, 2000), p. 235.
- ⁷H. J. Fitting, T. Barfels, A. N. Trukhin, and B. Schmidt, J. Non-Cryst. Solids **279**, 51 (2000).
- ⁸R. Tohmon, H. Mizuno, Y. Ohki, K. Sasagane, K. Nagasawa, and Y. Hama, Phys. Rev. B **39**, 1337 (1989).
- ⁹H. Nishikawa, E. Watanabe, D. Ito, and Y. Ohki, Phys. Rev. Lett. **72**, 2101 (1994).
- ¹⁰H. Imai, K. Arai, H. Imagawa, H. Hosono, and Y. Abe, Phys. Rev. B **38**, 12 772 (1988).
- ¹¹G. Pacchioni and G. Ieranó, Phys. Rev. Lett. **79**, 753 (1997).
- ¹²V. Sulimov, S. Casassa, C. Pisani, J. Garapon, and B. Poumellec, Modell. Simul. Mater. Sci. Eng. **8**, 763 (2000).
- ¹³M. Busso, S. Casassa, C. Pisani, and V. Sulimov, Modell. Simul. Mater. Sci. Eng. **10**, 21 (2002).
- ¹⁴V. B. Sulimov, P. V. Sushko, A. H. Edwards, A. L. Shluger, and A. M. Stoneham, Phys. Rev. B **66**, 024108 (2002).
- ¹⁵L. Skuja, J. Non-Cryst. Solids **239**, 16 (1998).
- ¹⁶L. Skuja, J. Non-Cryst. Solids **149**, 77 (1992).
- ¹⁷L. Skuja, A. N. Streletsky, and A. B. Pakovich, Solid State Commun. **50**, 1069 (1984).
- ¹⁸B. L. Zhang and K. Raghavachari, Phys. Rev. B **51**, 7946 (1995).
- ¹⁹V. B. Sulimov and V. O. Sokolov, J. Non-Cryst. Solids **191**, 260 (1995).
- ²⁰D. Donadio, M. Bernasconi, and M. Boero, Phys. Rev. Lett. **87**, 195504 (2001).
- ²¹S. Agnello, R. Boscaino, M. Cannas, F. M. Gelardi, M. Leone, and B. Boizot, Phys. Rev. B **67**, 033202 (2003).
- ²²C. J. Brinker and G. W. Scherer, *Sol-Gel Science* (Academic, New York, 1989).
- ²³K. M. Davis and M. Tomozawa, J. Non-Cryst. Solids **201**, 177 (1996).
- ²⁴J. C. Mikkelsen, Appl. Phys. Lett. **39**, 903 (1981).
- ²⁵T. Bakos, S. N. Rashkeev, and S. T. Pantelides, Phys. Rev. B **69**, 195206 (2004).
- ²⁶G. Ghosh, *Handbook of Thermo-Optic Coefficient of Optical Materials with Applications* (Academic, New York, 1998).
- ²⁷A. E. Geissberger and F. L. Galeener, Phys. Rev. B **28**, 3266 (1983).
- ²⁸N. Chiodini, F. Meinardi, F. Morazzoni, A. Paleari, R. Scotti, and G. Spinolo, Solid State Commun. **109**, 145 (1999).
- ²⁹V. Gottardi, M. Guglielmi, A. Bertoluzza, C. Fagnano, and M. A. Morelli, J. Non-Cryst. Solids **63**, 71 (1984).
- ³⁰M. A. Garcia, S. E. Paje, M. A. Villegas, and J. Llopis, Mater. Lett. **43**, 23 (2000).
- ³¹J. Lin and K. Baerner, Mater. Lett. **46**, 86 (2000).
- ³²A. Anedda, C. M. Carbonaro, F. Clemente, R. Corpino, F. Raga, and A. Serpi, J. Non-Cryst. Solids **322**, 95 (2003).
- ³³N. Chiodini, F. Meinardi, F. Morazzoni, A. Paleari, R. Scotti, and D. Di Martino, Appl. Phys. Lett. **76**, 3209 (2000).
- ³⁴F. Meinardi and A. Paleari, Phys. Rev. B **58**, 3511 (1998).
- ³⁵G. Pacchioni and G. Ieranó, J. Non-Cryst. Solids **216**, 1 (1997).
- ³⁶D. Donadio, Master's thesis, University of Milano-Bicocca, 2000.
- ³⁷N. F. Mott, Proc. R. Soc. London, Ser. A **167**, 384 (1938).
- ³⁸C. W. Struck and W. H. Fonger, J. Lumin. **10**, 1 (1975).
- ³⁹O. A. Zhikol, A. F. Oshkalo, O. V. Shishkin, and O. V. Prezhdo, Chem. Phys. **288**, 159 (2003).